2nd CARL LOPER CAST IRON SYMPOSIUM
Latest advances and applications of cast iron

Ultrafine spheroidal graphite iron castings by use of thin-walled permanent molds

* Haruki Itofuji[1*], Kazuya Edane[2], Takehiro Sakatani[3], Masayuki Itamura[1]

1* I2C Technology Institute, Ube 755-0025, Japan

2 Tsuchiyoshi Industry Co., Ltd., Onan 696-0403, Japan

3 Yoshiwa Kogyo Co., Ltd., Aki 736-0056 Japan

KEYWORDS

ultrafine
spheroidal graphite
thin wall
permanent mold
gravity die cast
as cast

Each keyword starts on a new line
Write up to 6 keywords

ABSTRACT

In this study, gravity die casting of spheroidal graphite iron had been attempted controlling free nitrogen during preparing base molten iron, magnesium treatment, inoculation and pouring. The actual CO/SiO_2 reaction temperature of base molten irons was measured and magnesium treatment was conducted at that temperature using a low nitrogen contained spheroidizer agent. The size of cavity in the mold was thickness of 5.4mm and diameter of 35mm and the mold was made of a 0.5 mass% carbon steel. This resulted in ultrafine graphite nodules obtained without any chill in the as-cast condition. The nodules were an average diameter of 7μm and density count of over 3,000 n/mm². An automotive steering knuckle was also cast using the same procedure. The knuckle had no major defects like shrinkage, chill etc. in as-cast conditions. The possibility of no chill in this study has become extremely higher than former study. The tensile properties showed good improvement than that in conventional values. The study was based on the free nitrogen theory for the chilling besides the site theory as graphite spheroidization.

1. INTRODUCTION

In last four decades, spheroidal graphite iron castings have been increased in their production quantity like graph rising to the right in industrialized countries. The example in Japan is shown in Fig. 1[1)]. From the viewpoint of the material development, if the nodule size of spheroidal graphite can be controlled an extremely small by fast cooling like permanent mold casting, the mechanical properties such as tensile, fatigue limit strength and fracture toughness will be expected higher values than current sand mold castings[2)]. Furthermore, new physical property such as high thermal conductivity may be expected because graphite nodule spacing is much narrower than that of present spheroidal graphite irons. As the results, new usage will be found, and it will be adopted in wider fields than now and the production quantity will increase continuously in future.

On the other hand, the labor environment and the productivity have not improved so much since the molds have been made of sands conventionally. It is dusty, dark and hot in foundry. It needs the wide area of sand facility and cooling bed. These are unfavorable factors for not only labors but also foundry managers. If permanent mold casting was possible, they would be able to be solved mostly in manner like breakthrough in aluminum die casting.

Many researchers[4-10)] had tried permanent mold casting for spheroidal graphite iron to not only develop a new material but also create a future model of iron foundry. However, the permanent mold casting in spheroidal graphite iron castings brings to chill structure (cementite; Fe_3C) therefore such castings must be conducted heat treatment for graphitization. There had been almost no foundry who could succeed chill free castings in as-cast condition in practice although some researcheres[7-9)] had been able

* *Haruki Itofuji*. Tel.: +81-80-5620-4938. E-mail address: h.itofuji@keb,biglobe.ne.jp

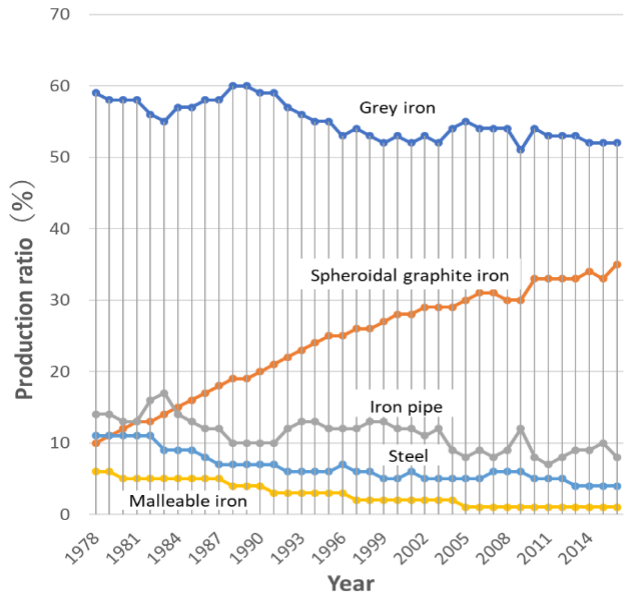

Fig.1 Production ratio of ferrous castings for last four decades.

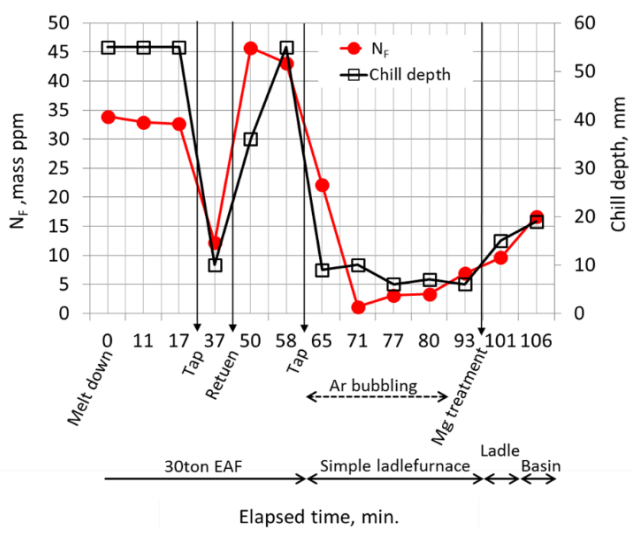

Fig.2 Relationship among chill depth and molten conditions in spheroidal graphite iron

to succeed it in laboratory.

According to author's study[11], it has been clear that free nitrogen N_F in molten iron and chill depth in wedge sample have good relationship as shown in Fig. 2. The other factors do not show the clear relationship. It has been considered that nitrogen atom can partially substitute carbon atom in cementite crystal structure (Fe_3C) and enhances chill formation when the solidification rate is fast enough. Such cementite might be the form of $Fe_3(C \cdot N)$. If the Table 1 Chemical composition of raw materials for gravity die casting. denitrification could be conducted properly, there will be no chill structure in permanent mold casting too. Finer nodule size will be expected as the results because of fast cooling rate.

Table 1 Chemical composition of raw materials for gravity die casting.

Raw material	Chemical composition (mass %)					
	C	Si	Mn	P	S	Al
Pig iron	3.69	1.02	0.11	0.025	0.006	0.009
Fe-Si	0.10	75.03	—	0.026	0.004	1.34
Fe-S	—	—	—	—	48.76	—
Carbon	99.24	—	—	—	0.026	—

In this study, permanent mold casting of spheroidal graphite iron was attempted to get ultrafine graphite nodule under stable conditions in laboratory and to apply the technology in practice.

2. EXPERIMENTAL PROCEDURE

The raw materials for gravity die castings shown in Table 1 were melted using a 30kg high frequency induction furnace. Melting, magnesium treatment, inoculation, and pouring were conducted using the time-temperature schedule shown in Fig. 3. The schedule had been already reported to countermeasure chill formation[12] but changed a little for this study. After being melted, the base molten iron was super-heated at over 1,500℃ and slowly cooled down to the equilibrium CO/SiO_2 reaction critical temperature T_{EC} without electric power. During cooling down, chill sample was taken with general permanent mold and chemical composition was analysed using spectrometer. T_{EC} was calculated according to the carbon and silicon contents in the base molten iron, according to Eq. (1) and (2)[13].

$$T_{EC}\,(℃) = T_K - 273 \quad \cdots\cdots\cdots\cdots\cdots\cdots (1)$$

$$T_K = -27{,}486 / (\log[Si/C^2] - 15.47) \quad \cdots\cdots\cdots (2)$$

Around calculated T_{EC}, the starting temperature of SiO_2-film formation on the surface of base molten iron, so-called the actual

CO/SiO_2 reaction critical temperature T_{AC} was measured using K-type thermocouple. During slow cooling, denitrification was expected by solution difference of nitrogen in temperature decrease[8]. At around the temperature of T_{AC}, electric power was off or minimized not to let molten iron stirring. Magnesium treatment was conducted at T_{AC} using a plunger in the furnace (Fig. 4). Stream inoculation was conducted during tapping in alumina-silica ceramic ladle after magnesium treatment (Fig. 4). These chemical compositions and amount of treatments are shown in Table 2. To make treatment reaction mild, alloy should have lower magnesium content as possible because the alloy contained high magnesium cause intense reaction and promote chill[9]. The magnesium-treated and inoculated molten iron was poured into the preheated permanent mold using an alumina-silica ceramic spoon within 30s after inoculation. The pouring temperature aimed was 1320 ± 20℃. The shape and dimensions of the permanent mold[12] is shown in Fig. 5. This die was originally designed and manufactured to take chill samples for accurate spectrometry analysis in general foundry operations.

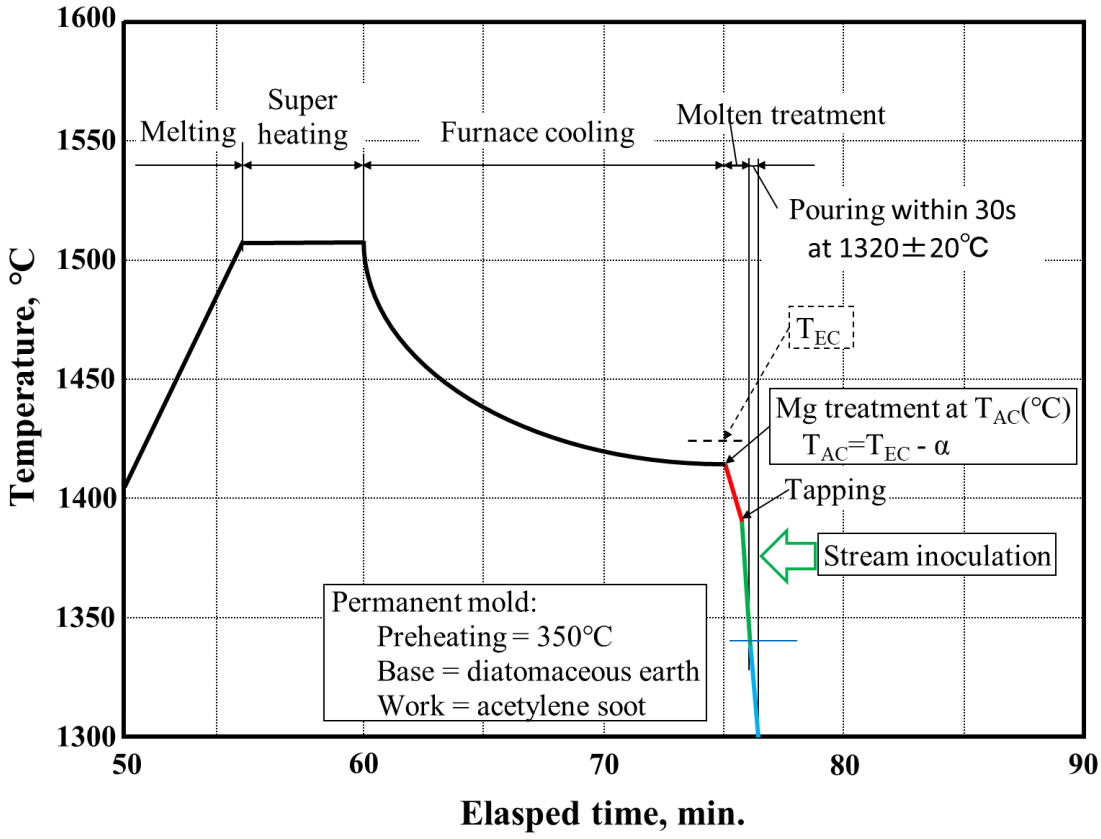

Fig. 3 Time-temperature schedule for melting, molten treatment and pouring.

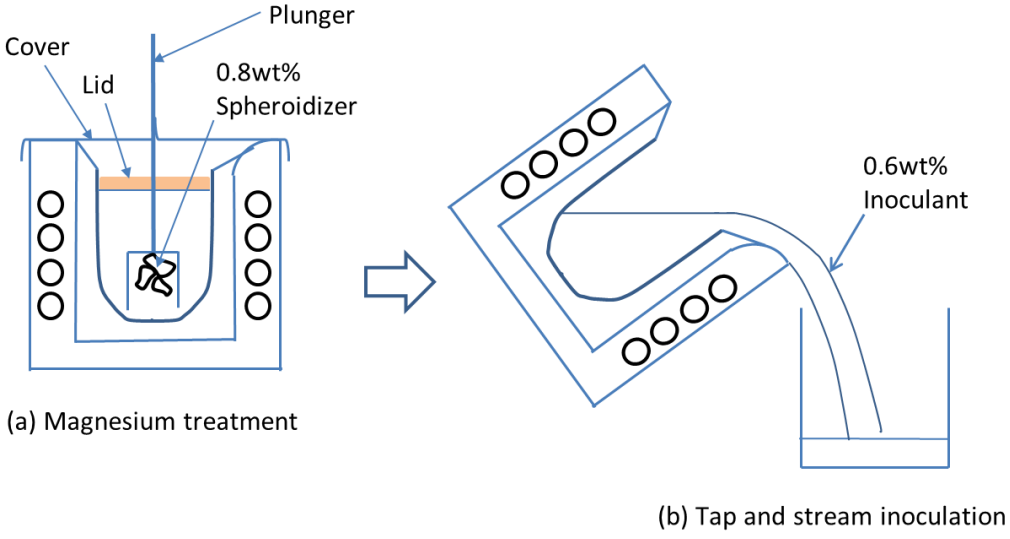

Fig. 4 Procedure of magnesium treatment and inoculation

Table2 Chemical composition of Fe-Si base agents and amount of their additions.

Mold	Agent	Chemical composition (mass %)						Chemical composition (mass ppm)		Add. (wt.%)
		Si	Mg	Ca	RE	Al	C	O	N	
Perma.	Mg alloy	44.1	3.9	0.7	1.4	0.4	2.0	767	8	0.8
	Inoculant	75.8	—	1.8	—	2.2	—	347	41	0.6
Sand	Mg alloy	45.5	5.8	2.1	2.4	0.3	—	515	893	1.1
	Inoculant	76.2	—	1.8	—	2.2	—	3542	46	0.4

Table 3 Chemical composition of raw materials for sand mold castings.

Raw material	Chemical composition (mass %)					
	C	Si	Mn	P	S	Al
Pig iron	4.17	0.26	0.03	0.027	0.015	tr.
Steel scrap	0.01	1.11	0.19	0.011	0.008	tr.
Fe-Si	0.05	75.70	tr.	0.015	0.005	1.27
Fe-Mn	6.73	0.36	76.50	0.120	0.017	tr.
Fe-S	—	—	—	—	48.76	—
Carbon	99.24	—	—	—	0.026	—

The permanent mold was coated with two layers. One was the base coating which was directly coated on the die. It was water-based diatomite. The thickness was about 0.4mm. Another was the work coating on the base and was acetylene soot. The thickness was about 0.2mm. Coated permanent mold was preheated to 350℃ in an electric holding furnace. The as-cast sample castings were taken out at temperature below 550℃. The three-dimensional illustration of sample is also shown in Fig. 5. Chill samples for spectrometer were taken by pouring the same liquid iron into general permanent mold. The chemical composition was analysed using spectrometry. This spectrometry has a pulse-height distribution analysis (PDA) system and state analysis of magnesium[14] could be conducted. The analysis samples were also analysed on carbon and sulfur contents using the infrared absorption method (CS-LS600, Leco Corp.).

A sample casting was cut in the vertical section from gate to bottom. It was buried in resin and the microstructures were observed using optical microscopy. SG_S was measured and SG_N were counted through the microstructural photograph by hand.

Three different kind of sand mold castings were poured. Their microstructures were compared with die castings. The first was wall thickness of 6.5mm and weight of 130kg which would be able to show the maximum graphite nodule count in conventional technology. The second was 25mm Y type block which was described in JIS G 5502. The microstructure was used as standard. The raw materials for sand mold castings shown in Table 3 were melted for these castings using 10ton low frequency induction furnace.

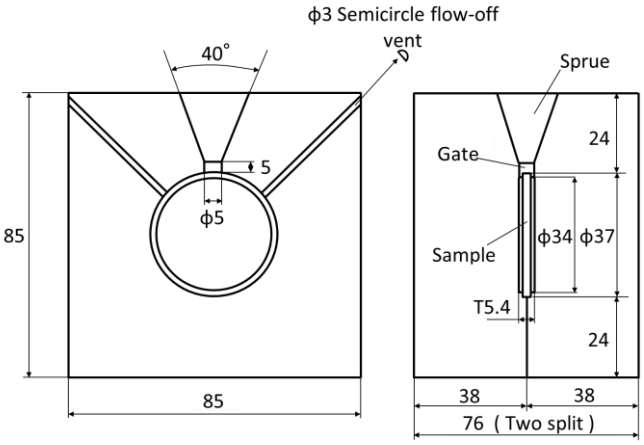

(a) Dimension of permanent mold

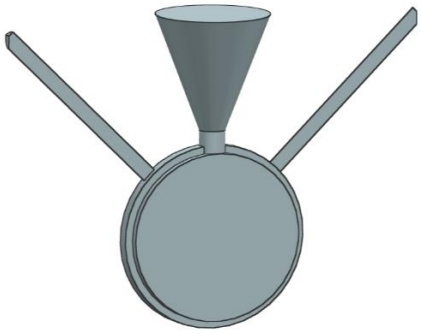

(b) Shape of sample

Fig. 5 S50C permanent mold and sample

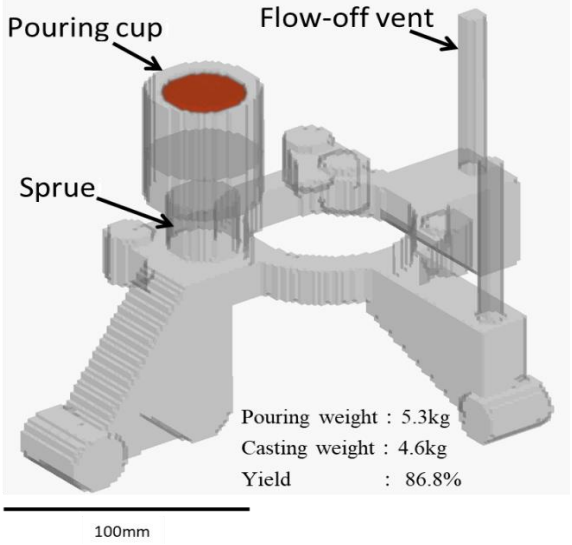

Fig. 6 Cast design of steering knuckle for automobile which was deformed for this study.

The alloys shown in Table 2 were used for liquid treatment. The third was wall thickness of 230mm and weight of 36,000kg which the solidification time was controlled within 150minites using chillers. This would be shown as a typical microstructure of heavy section castings which the mechanical properties were guaranteed. The casting was die-plate for injection machine[15].

Although the same raw materials and alloys were added, 30ton electric arc furnace was used in this case.

To consider the possibility of chill free gravity die casting in spheroidal graphite iron in practice, a steering knuckle for automobile was also poured taking the same procedure as described above. The riserless casting design is shown in Fig. 6. A gating system was not designed but the sprue was connected directly to the knuckle body. The quality was surveyed about the surface, the shrinkage, the microstructure and the tensile properties.

3. RESULTS

The chemical compositions of the molten irons are shown in Table 4. T_{EC} of the base molten iron was calculated as 1425℃ by Eqn. (1) and (2). After the base molten iron was super-heated to 1540℃, it was slowly cooled down in the furnace without electric power. SiO_2 film began to form at about 1415℃ when carbon and silicon were 3.66 and 2.58mass% respectively. Magnesium treatment was conducted at 1415℃ using plunger in the furnace. The difference between T_{EC} and T_{AC} was about 15℃. Soon after the magnesium reaction finished, the molten iron was tapped into ceramic ladle. Stream inoculation was conducted during tapping. The treated molten iron was poured into the preheated die at 1340℃ using the ceramic spoon. The time elapsed from inoculation to pouring was 23sec. These conditions are shown in Table 5 compering with other heats. Polished cross section of sample casting is shown in Fig. 7. A depression on the side wall and inside shrinkages were observed as shown in Fig. 7A when sample castings were no chill and full graphite structure. When some conditions were wrong, chill macrostructure was observed as shown in Fig. 7B. The chemical composition of the magnesium-treated and inoculated molten irons is also shown in Table 4. Carbon and sulfur values in analysis samples after these treatments showed less accuracy in spectrometry analysis. According to the former study[12], it was considered that graphite precipitation was rather dominant although molten iron was poured into general die for full chill. Therefore, the analysis results of the infrared absorption method were adopted for them in Table 4. The results of state analysis are also shown in Table 4. Mg_F is metallic state of magnesium[14]. Mg_T is total magnesium[14] and is called as residual magnesium in conventional foundry operations.

Full spheroidal graphite structure was observed in gravity die cast sample. The representative microstructure is shown in Fig. 8. Most of spheroidal graphite was ultrafine (Fig. 8(a)). The range of SG_D was 4~9μm and the average SG_D was 7μm. Larger spheroidal graphite nodules exist but their diameters remain at about 15μm. These were assumed to be hypereutectic graphite nodules that formed during pouring. SG_N was 3220 count/mm^2. Fine shrinkage cavities were found beneath the depression on the side wall of the sample casting. This might be caused by the narrow gate. Since magnesium treatment was conducted at T_{AC}, success rate of full graphite structure could be much better than that of former study[12].

Table 4 Chemical composition of molten irons.

Mold	Sample		Chemical composition (mass %)							
	castings (mm)	Chill	C	Si	Mn	P	S	Mg_F	Mg_T	CE
Permanent	t5.4 x φ34	Base	3.66	2.58	0.09	0.022	0.006	—	—	4.52
		After treatment	3.61	3.11	0.10	0.024	0.008	0.013	0.018	4.65
	Steering knuckle	Base	3.46	2.59	0.07	0.020	0.013	—	—	3.32
		After treatment	3.40	3.26	0.07	0.020	0.009	0.016	0.020	4.49
Sand	t6.5 Thin wall box	Base	3.69	2.60	0.51	0.047	0.041	—	—	4.56
		After treatment	3.51	3.65	0.53	0.047	0.017	0.036	0.043	4.73
	25-Y block	Base	3.55	1.48	0.21	0.039	0.020	—	—	4.04
		After treatment	3.42	2.66	0.21	0.038	0.013	0.031	0.037	4.31
	t230 Die-plate	Base	3.54	1.44	0.26	0.040	0.010	—	—	4.02
		After treatment	3.46	2.36	0.28	0.045	0.007	0.038	0.043	4.25

t = Wall thickness, Mg_F = Free magnesium = Metallic magnesium
Mg_T = Total magnesium = Residual magnesium, CE = C + 1/3Si

Table 5 Condition of melting, molten treatment and pouring in each heat.

Mold	Sample (mm)	Temperature (°C)						Elasped time* (sec.)
		Super heating	T_{EC}	T_{AC}	Mg treatment	Inoculation	pouring	
Permanent	t 5.4 x Φ34	1540	1425	1409	1410	1386	1324	23
	Steering knuckle	1517	1426	1410	1412	1374	1326	38
Sand	t 6.5 Thin wall box	1507	1425	1408	1461	1461	1417	59
	25 Y-block	1483	1403	1387	1405	1405	1335	137
	t 230 Die-plate	1525	1402	1387	1398	1398	1324	900

* Elasped time = Fading time after Mg treatment and inoculation

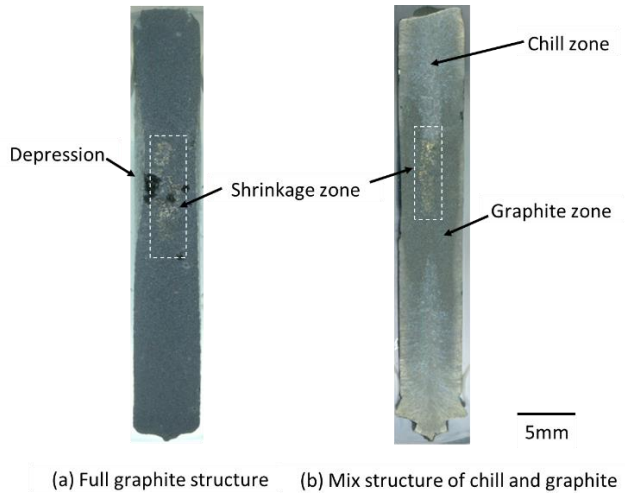

Fig. 7 Polished cross-sectional surface of t5.4 x Φ34 as-cast sample castings (3vol.% Nital etch).

Chill (ledeburite) was only observed in the Φ3.0mm semicircle flow-off vent. The microstructure is shown in Fig. 9. SG_N was 3620 count/mm^2. To compare the microstructures in conventional sand castings, three kinds of the microstructures were also shown in Fig. 8(b)~(d). This comparison is simple and easy to understand. The microanalytical results are shown in Table 6. The microstructure shown in Fig. 8(b) is close to the conventional limit of nodule density without chill.

The steering knuckle was poured into preheated die at 1326℃. The time elapsed between inoculation and pouring was 38s. The filling time was 6s. The knuckle was taken out from the mold at a temperature below 500℃. The as-cast appearance of the steering knuckle is shown in Fig. 10(a). The surface appears good without any visible magnesium dross, flow marks, cold shot, or other defects. The knuckle was cut at the position A, B, and C in Fig. 10(a). The sectional surfaces were visually observed. The results are shown in Fig. 10(a)~(d). No shrinkage was observed in any sections. However, a slight degree of gas holes was observed on the surface in section A and C. The nodule number density reached over 2240 count/mm^2. As an example, the microstructure of section B in the steering knuckle is shown in Fig. 11. This count was over 10 times greater than that found in similar size of sand mold steering knuckles[16]. No chill was observed. The microanalytical results are shown in Table 6. The results of tensile test in the knuckle is shown in Table 7. All the tensile properties exceeded more than the values required.

4. CONSIDERATIONS

When wall thickness becomes thinner and/or cooling rate become faster, SG_D generally becomes smaller and SG_N increases. However, ledeburite structure begins to form when the cooling rate is too fast. According to H. Horie[3], the critical count of SG_N without any ledeburite structure is approximately 900 count/mm^2 giving Eq. (3):

$$SG_N = 0.58R2 + 19.07R + 1.01 \cdot \cdot \cdot \cdot \cdot \cdot \cdot (3)$$

where

R = Cooling rate (℃/s)

R is about 26.2℃/s when SG_N is 900 count/mm^2. In this study, the critical SG_N was considered between 3200 and 3600 count/mm^2. Therefore, the cooling rate might be 60-62℃/s. This is a substantial difference from conventional studies. The difference may arise from the theory which N_F onto implication of chill (Fe_3C) formation is imaged or not. N_F control is the key point in this study. N_F can be reduced by slowly cooling from the superheating temperature and can be further offset by the addition of inoculant including elements such as aluminum, calcium, and silicon.

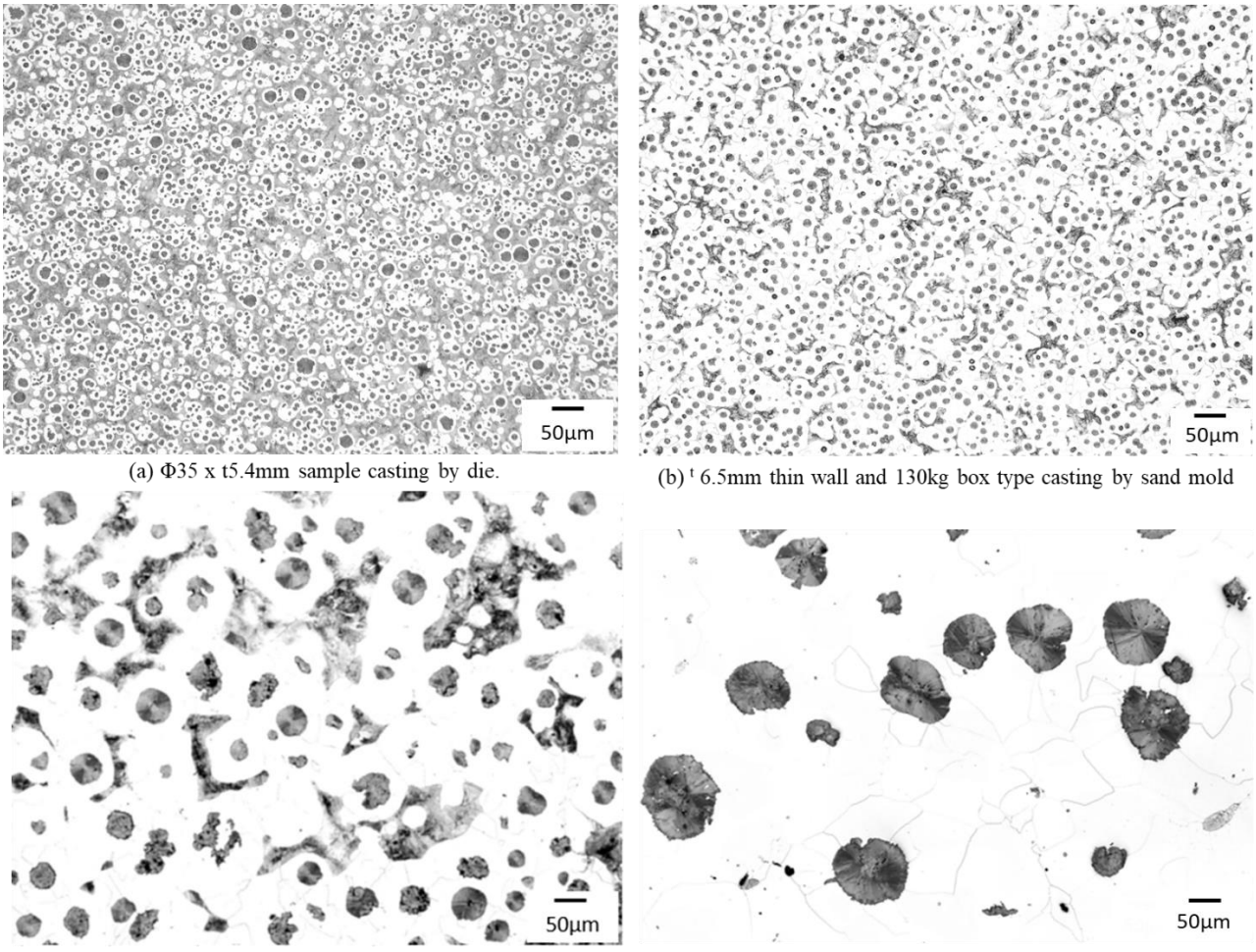

(a) Φ35 x t5.4mm sample casting by die.

(b) t 6.5mm thin wall and 130kg box type casting by sand mold

(c) 25㎜ standard Y-block (JIS G 5502-2001) by sand mold[14)]

(d) Heavy section of 230mm in 36ton die plate cast by sand mold with chillers[15)]

Fig. 8 Microstructures of permanent and sand mold castings (3vol.% natal etch)

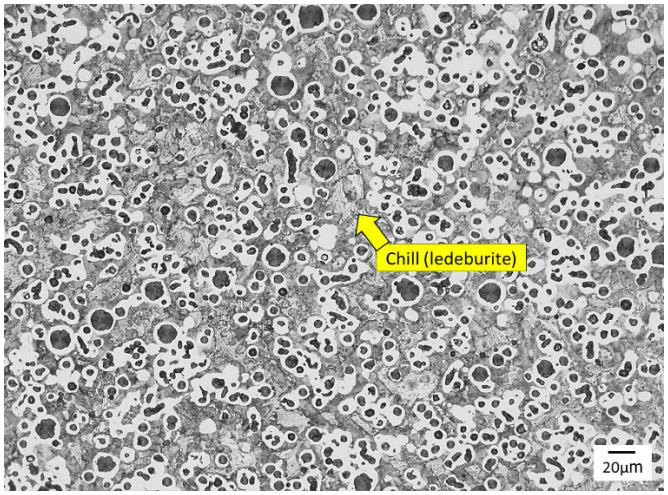

Fig. 9 Microstructure of flow-off vent for permanent mold casting (3vol.% natal etch). SG_N; 3620 count/mm^2

The good relationship between N_F and chill depth in wedge-sample was previously proved by the authors and successfully applied in foundry practices[11)].

Alloying elements such as manganese and chromium are generally known to promote chill formation tendencies[17)]. These elements are also known to increase nitrogen resolution in molten iron [18)]. On the contrary, carbon, silicon and phosphorus decrease increase nitrogen resolution in molten iron and inhibit chill formation[17,18)]. This suggests that they may promote chill by increasing N_F levels in molten iron. Such elements may promote chill as the atoms substituting for iron atoms in Fe_3C because they are close to in atomic size. Furthermore, the electronegativity of such substitution elements with carbon is greater than that between iron and carbon [8)]. The same is true for nitrogen and oxygen atoms regarding substitution. N_F and chill are related by the substitutional ability of nitrogen atoms for carbon atoms in Fe_3C, which could promote chill. However, free oxygen (O_F) has less possibility to promote chill according to the results of the previous study [11)]. Sulfur is effective

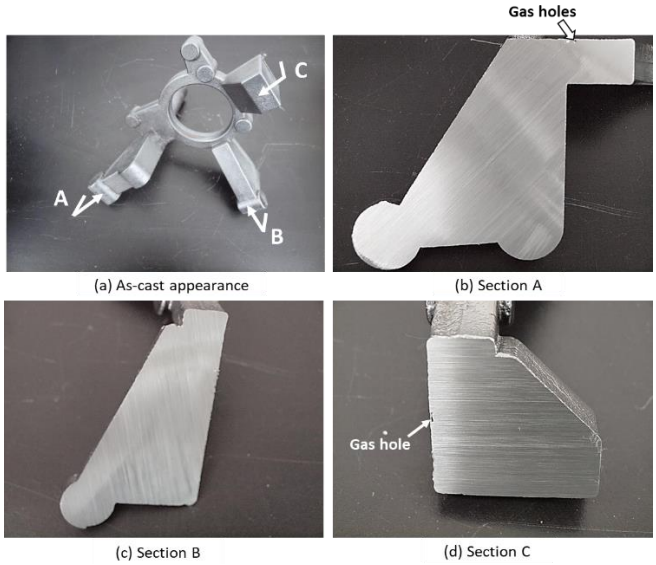

Fig. 10 Quality of surface and cross-sections in steering knuckle by gravity die casting.

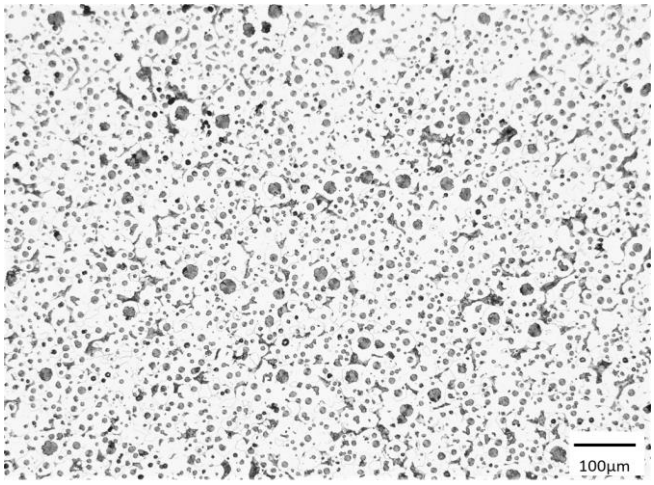

Fig. 11 Microstructure of surface layer at section B in steering knuckle, as shown in Fig. 10(a) (3vol.% natal etch).

Table 6 Results of microstructural analysis.

Mold	Sample (mm)	Diameter Ave.(μm)	Density (N/mm^2)	Nodularity (%)	Perlite (%)
Permanent	t 5.4 x Φ34	7	3220	94	70
	Steering knuckle	9	2240	97	5
Sand	t 6.5 Thin wall box	15	889	98	20
	25 Y-block	38	111	87	25
	t 230 Die-plate	110	15	93	2

N = Number of count

Table 7 Results of tensile test at section B in steering knuckle, as shown in Fig. 10(a).

Sample		0.2% proof stress (Mpa)	Tensile strength (Mpa)	Elongation (%)	Reduction of area (%)
Value required		≧250	≧390	≧15	—
Knuckle	①	312	523	18	8
	②	378	525	19	9
	③	375	524	18	8

Table 8 Calculated diameter of magnesium gas bubbles in molten iron.

Temperature (℃)	Vapore presure (atom)	Bubble diameter (μm) at molten iron depth D (cm)			
		D = 1	D = 10	D = 100	D = 500
1300	4.15	17	17	21	*
1350	5.64	12	12	13	40
1400	7.53	8	8	9	16
1450	9.89	6	6	7	10
1500	12.79	5	5	5	6
1550	16.32	3	3	4	4
1600	20.54	3	3	3	3

to inhibit nitrogen absorption and chill formation[19], but it inhibits graphite spheroidization.

Magnesium vapors at about 1100℃ in atmospheric pressure. The magnesium atom has almost no solubility in molten iron. Therefore, vapored magnesium gas can exist as gas bubbles in molten iron. The size of magnesium gas bubbles is calculated by Eq. (4)[20] and (5). The calculated diameter of magnesium gas bubbles is shown in Table 8. Spheroidal graphite nodule shown in Fig.11 in this study had the average size of 7μm. This is close to calculated size of magnesium gas bubbles in molten iron when the magnesium alloy is treated at 1400–1450℃ (Table 8) [21]. According to Table 8, finer magnesium gas bubbles would be able to be possible in shallower molten depth and/or higher temperature than this study, if there were other way to have chill free in as-cast condition.

Vapor pressure of magnesium(atm) : P_{Mg}

$$\text{Log } P_{Mg} = 4.958 - (1.229 \times 104)/T \quad \cdots\cdots (4)$$

T ; Rankine temperature= 1.8 x Absolute temperature K

Diameter of magnesium gas bubble(μm) :D

$$P_{Mg} = Pa + \rho gH + 4\gamma/D \quad \cdots\cdots (5)$$

$$D = 4\gamma/(P_{Mg} - Pa - \rho gH)$$

Pa: Atmospheric pressure(1atm)

ρ: Density ($6.8 g/cm^3$)

g: Gravitational acceleration(980cm/s2)

H: Hight of molten iron (cm)

γ: Surface tension(1450dyne/cm)

P. Kainzinger, et.al[22] had concluded that fatigue limit strength improves when the density count of spheroidal graphite become smaller in sand mold casting. Since the range of density count was 20~250count/mm^2 in their study, the great improvement of fatigue limit strength may be expected density count like this study. The results of the tensile test make design engineers expect a much higher fatigue limit strength value than conventional spheroidal graphite iron castings. Furthermore, higher thermal conductivity may be expected than that of conventional spheroidal graphite iron because the mutual distance among nodules are much closer than that of conventional one.

Besides nodule size and density count, full graphite structure with no chill in knuckle casting in as-cast condition must be trustworthy. There were some laboratories[7,9,23,24] who had succeeded permanent mold spheroidal graphite iron castings without heat treatment, but there was almost no report for applying it in foundry practice yet. There are some foundries[5,6,25] who have taken permanent mold casting of spheroidal graphite iron. However, they have had graphitization heat treatment of ledeburite structure. It has been known that graphitization heat treatment of chill irons contained magnesium completes in a short time such as a quarter hour. This is much shorter than that of malleable irons. But there is a possibility to form an unfavorable microstructure such as low nodularity, nodule line-up like discontinuous crack, etc.[10]. These unfavorable microstructures depend on the distribution of magnesium voids. Magnesium voids exist the site between cementite and austenite in needle like ledeburite[21]. The sphere shape of magnesium gas bubbles becomes irregular by ledeburite when molten iron solidifies. Tempered graphite precipitates in magnesium voids[7]. Graphite line-up may affair the mechanical properties, especially fatigue limit strength.

It was confirmed that the N_F theory[11,12,26] for chill formation and the site theory[27-30] for graphite spheroidization could be used practically to get ultrafine spheroidal graphite iron casting with no chill in as cast condition. As the issues in next study, N_F shall be analyzed as the same procedure as former study[11].

5. CONCLUSIONS

Gravity die casting of spheroidal graphite iron was attempted controlling N_F. The following results were concluded:

(1) For both the sample and steering knuckle castings, chill free and full graphite structures could be obtained in as-cast condition.
(2) The average SG_D were 7μm in t 5.4 XΦ34mm casting and 9μm in Knuckle casting. They had been never reported by other researchers before.
(3) On the magnesium treatment temperature as one of conditions to get full graphite structure, T_{AC} was more stable condition than T_{EC}.
(4) New adoption of ultrafine spheroidal graphite iron castings may be expected for industrial use.

REFERENCES

1) Sokeizai center; Material yearbook (2017)
2) P.Kainzinger und F.Grun; Giesserei Rundschau 61(2014)Nr.11+12, s347~351
3) H. Horie; Imono 67 (2) (1995) 124-132.
4) H. Sakurai, M. Kawasaki, K. Ozaki; Technical Paper 945189, FISTA Congress (1994).
5) Y.S. Lerner; Foundry Management & Technology, Oct. (2003) 18-22.
6) A. Urrestarazu, J. Sertucha, R. Suarez, I. Alvarez-Ilzarbe; Rev. Metala. 49 (2013)325-339.
7) Y. Lee, et al.; Imono 55 (1983)156-163.
8) N. Inoyama, S. Yamamoto, Y. Kawano; Cast Irons clarified Through Bonds and Reactions (1992).
9) T. Kitsudou, K. Ashida, K. Fujita; Imono 62 (1990) 359-364.
10) Permanent Mold Casting of Irons; Japan Foundry Society (1976)
11) H. Itofuji, M. Tamura, Moritake, M. Itamura, K. Anzai; Imono,163th conference (2013) 99.
12) H. Itofuji, K. Kazuya, T. Kotani, M. Itamura, K. Anzai; Proceedinds of CastTec2016 (2016)
13) B. Marineki; Modern Casting, 42 (6) (1962) p99.
14) H. Itofuji, K. Kawamura, N. Hashimoto, H, Yamada; AFS Trans.,98(1990)585-595.
15) H. Itofuji;Int. J. Cast Metals Res. 12 (1999)179-187
16) K. Edane, Y. Ameku, Y. Kurokawa, H. Itofuji, M. Itamura, K. Anzai; Imono,168th conference (2016) 151
17) K. Taniguchi; Tetsu-to-Hagane18 (1932)952-980.
18) R.D. Pehlke; Trans. Met. Soc. AIME, 218 (1960)1088.
19) T. Choh, M. Inoue; Tetsu-to-Hagane 54(1968)19
20) P.K. Trojan, R.A. Flinn; Trans. ASM,54(1961)549-566
21) H. Itofuji;Int. J. Cast Metals Res., 17 (2004)220-228
22) P. Kainzinger und F. Grun; Giesserei Rundschau 61(2014) Nr.11+12, s347~351
23) M. S. C. Rao, M. N. Srinivasan; AFS Trans.,96(1988) 79-89
24) K. G. Davis, J. G. Magny, D. A. Brown and D. Hui; Advanced Casting Technology, Proc. Conf. Kalamazoo, MI Nov 12- 14 (1986)221-230.
25) H. Sakurai, M. Kawaguti and K. Osaki; The Integration of Design and Manufacture (1994)55-61
26) H. Itofuji, K. Edane, Y. Kurokawa, M. Itamura, K. Anzai; Imono,168th conference (2016) 148.
27) H. Itofuji;Thesis of Kyoto University (1993).
28) H. Itofuji; AFS Trans.,104(1996)79-87
29) H. Itofuji; Imono, 84(2012)194-202
30) H. Itofuji; Imono, 90(2018)587-593

ACKNOWLEDGEMENT

Authors wish to express our sincere gratitude to Professor Koichi Anzai for his supervision, helpful suggestion and continual encouragement throughout this study.